Available online at www.sciencedirect.com

ScienceDirect

Procedia CIRP 94 (2020) 531–536

www.elsevier.com/locate/procedia

11th CIRP Conference on Photonic Technologies [LANE 2020] on September 7-10, 2020

# Laser-assisted joining of AISI 304 thin sheets with polymers

Klaus Schricker[a,*], Alexander Drebing[a], Marc Seibold[a], Jean Pierre Bergmann[a]

[a] *Technische Universität Ilmenau, Department of Mechanical Engineering, Production Technology Group, 98693 Ilmenau, Germany*

* Corresponding author. Tel.: +49-3677-69-3808; fax: +49-3677-69-1660. *E-mail address:* info.fertigungstechnik@tu-ilmenau.de

**Abstract**

Laser-assisted metal-polymer joining gains importance in several applications due to the possibility of a direct connection between both materials. Aside from lightweight construction, a direct metal-polymer connection shows a high economic potential especially in large series production, e.g. domestic appliances. Based on this motivation, laser-assisted simultaneous joining of AISI 304 thin sheets (0.3…1.0 mm, X5CrNi18-10) with unreinforced polypropylene (PP) as well as acrylonitrile butadiene styrene (ABS) is carried out. Starting from a generally valid process description based on the energy per sheet thickness, the distortion as well as the mechanical properties are examined, whereby up to 17.4 MPa are reached and the tensile shear strength drops by at least 15 % during alternating climate test (-20…75 °C, 40…75 % rel. humidity). Further investigations under cyclic load showed, that long life fatigue strength ($5 \cdot 10^6$ cycles) is achieved at about 47 % of the initial tensile shear strength.



*Keywords:* laser welding; metal-plastic; metal-polymer; hybrid joint; hybrid joining; alternating climate test; fatigue; distortion; PP; ABS

## 1. Introduction and state of the art

The use of multi-material design is one of the leading issues in engineering constructions regarding functional integration and cost-efficiency. In this field, the combination of metals and polymers is a promising approach to meet the requirements combining materials with different properties. Especially in case of industrial applications for domestic appliances, steel sheets with thicknesses in the range from 0.3 mm up to 1 mm are widely used. On side of the plastic materials, unreinforced polymers are in the focus of interest and large-scale production relies mainly on thermoplastics manufactured by injection molding. Thereby, joining technology is a key parameter in creating multi-material components at a cost-efficient level. Especially in case of metal plastics joints, nowadays mostly adhesives or joining elements are used, with some restrictions, e.g. curing times or stress peaks. The named disadvantages of adhesive bonding and mechanical joining methods are avoided in laser-assisted joining [1] whereby cycle times below 15 s can be addressed.

For laser-assisted joining, the materials are arranged in overlap configuration. The metallic joining partner is heated, and the polymer melts due to heat conduction across the interface between both materials. This melted zone is now able to wet the metal surface and penetrate the surface structures [2]. Depending on the chemical structure of the polymer, the surface morphology and the structuring of the metal surface, a solid joint is formed after solidification [3].

The effect of surface preparation on tensile shear strength [4], distortion [5] and alternating climate test [6] is described for hybrid joints consisting of aluminum and steels with non-reinforced as well as fiber-reinforced polymers. Furthermore, investigations on fatigue are presented for ultrasonic welded [7] and friction welded [8] polymer-metal joints.

However, by addressing applications in the field of domestic appliance technology, thinner material thicknesses ($\leq 1$ mm) are coming to the fore, for which no comprehensive results are yet available.

In this contribution, laser-assisted joining of AISI 304 thin sheets with polypropylene (PP) as well as acrylonitrile butadiene styrene (ABS) is carried out under consideration of

2212-8271 
10.1016/j.procir.2020.09.177

the requirements of domestic appliance industry. Process-related investigations based on different laser beam powers, joining times and sheet thicknesses provide a general description of the joining process. The mechanical properties are then examined for different sheet thicknesses, whereby constant parameters are used for further investigations regarding alternating climate test and fatigue test. The investigations are concluded with a consideration of the distortion, which is of great interest for the addressed sheet thicknesses of the high-alloy steel below 1 mm and mainly induced due to the thermal joining process. Thus, a description of the relevant parameters and effects for the application of hybrid joints in domestic appliance technology is given.

## 2. Experimental setup

The experiments were carried out using a diode laser (Laserline LDM 1000) with a mean wavelength of 980 nm and a rectangular focus of 18·3 mm². The beam power $P_L$ was varied from 50 to 150 W. The clamping device used is described in detail in [9]. In terms of fundamental research, spot joints were manufactured in heat conduction joining and based on an overlap configuration of 100 mm length and 40 mm width (see Fig. 1). Joining times $\tau_L$ were used from 1 up to 8 s without applying inert gas supply. The high-alloy steel AISI 304 (comparable to X5CrNi18-10, $t_m$ = 0.3…1.0 mm) was chosen as metal joining partner. The metal surface was pre-treated by laser-structuring of grooves with a width of approx. 30 µm and a depth of approx. 40 µm by a pulsed fibre laser (Rofin PowerLine F20, see also [3]). On side of the thermoplastic, polypropylene (PP) and acrylonitrile butadiene styrene (ABS) were used with a thickness of 2 mm regarding the application in domestic appliances.

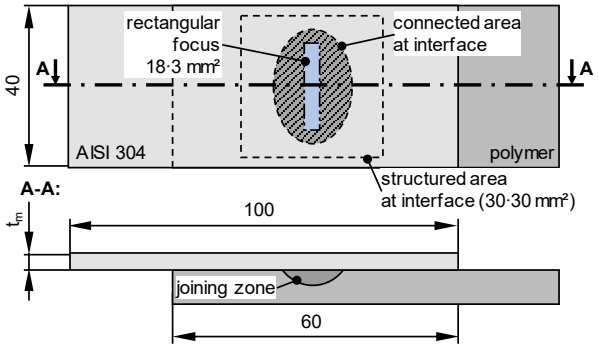


Fig. 1. Joint configuration of the metal-polymer hybrid

Based on the joining process, a melted zone is formed within the plastic material and evaluated regarding the area at the interface which is required to form the joint (see Fig. 1). This connected area was measured in fracture surfaces and depends on the laser beam power $P_L$, joining time $\tau_L$ and steel sheet thickness $t_m$, wherefore the energy per sheet thickness $E^*$ is introduced as combined parameter in equation (1). Microsections were taken from position A-A.

$$E^* = \frac{P_L \tau_L}{t_m} \quad (1)$$

Mechanical short-term test of tensile shear strength was performed using a universal testing machine (Hegewald Peschke 1455). The fatigue test was carried out on a Sincotec PowerSwing Mot Evolution 50 (stress ratio $R$ = 0.1) where the specimen is tested in natural frequency. The test was terminated when 5 million load cycles or a frequency drop of 3 Hz, which indicates the formation of cracks, was reached. Alternating climate tests were performed (-20…70 °C, 45…75 % rel. humidity, duty cycle: 26 h) up to 182 h (7 cycles). Distortion of the steel sheet was measured by photogrammetry using GOM Argus. A uniform size of the measuring field is implemented via number of points within the region of interest (approx. 3.5 million ± 10 %). The selected region prevents the inclusion of measuring errors at the sheet edges.

## 3. Results and discussion

### 3.1. Characterization of the joining process

A description of the joining zone is given by the connected area at the interface between steel and polymer. This area represents the load-bearing cross-section in which the polymer penetrates the surface structures. Fig. 2a shows the resulting connected area of PP depending the energy per sheet thickness $E^*$ to provide the general dependency between several sheet thicknesses, joining times and laser beam powers.

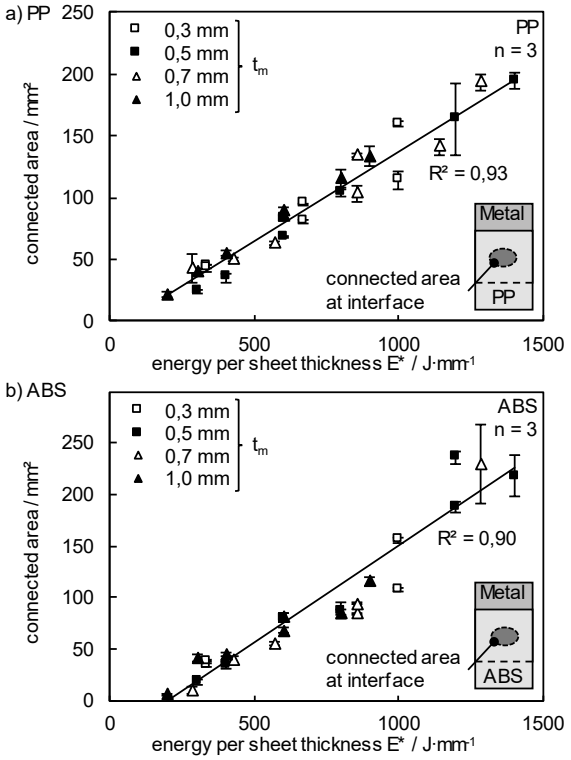


Fig. 2. Connected area at interface depending energy per sheet thickness E*for a) PP and b) ABS

The connected area increases linearly with rising $E^*$, whereby a coefficient of determination $R^2$ of 0.93 is reached by linear regression. ABS shows a comparable behavior achieving $R^2$ of 0.90 (see Fig. 2b). This characteristic response can be explained by the relatively low thermal conductivity of the

high-alloy steel, which is why the dissipated heat also increases linearly over the sheet thickness.

The relationship determined in the experiment between the connected area and the energy per sheet thickness $E^*$ can be explained by a simplified physical model (see Fig. 3). The formation of the joint requires an increase in temperature $\Delta T$ to the processing temperature of the polymer, for example the end of the melting interval $T_{em}$ for semi-crystalline materials [2]. This temperature also represents the maximum possible expansion of the connected area. The temperature increase can be calculated from the energy input $Q$, the mass $m$ and the specific heat capacity $c_p$ (2), whereby the energy input is given by the laser beam power $P_L$ multiplied by the joining time $\tau_L$ (3). The heated mass can be expressed as volume $V$ times density $\rho$ (4). The results of [11] are utilized to describe the volume V in a simplified way. It was shown by numerical simulation that the isotherms of the process temperature propagate almost perpendicular to the interface for comparable sheet thicknesses and joining times [11]. Thus, the volume $V$ of the heated material is considered simplified by the connected surface A multiplied by the sheet thickness $t_m$.

If these findings are plugged in (2) and rearranged according to the connected area $A$, equation (5) is obtained. Since the processing temperature $\Delta T$, density $\rho$ and specific heat capacity $c_p$ can be assumed to be constant for experiments with the same materials, equation (6) follows: The connected area $A$ is proportional to the ratio of $P_L$ times $\tau_L$ to $t_m$, defined as $E^*$.

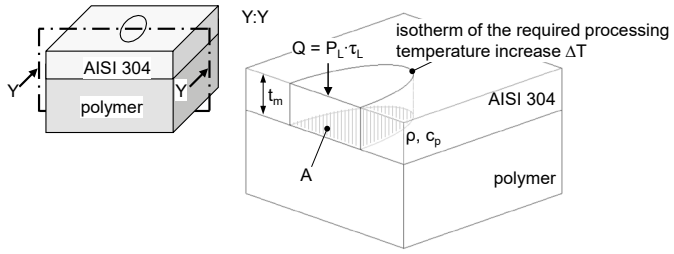


Fig. 3. Schematic representation of the simplified physical model to show the relationship between connected area A and energy per sheet thickness E*

$$\Delta T = \frac{Q}{mc_p} = \frac{P_L\tau_L}{t_m A\rho c_p} \quad (2) \qquad Q = P_L\tau_L \quad (3) \qquad m = V\rho = t_m A\rho \quad (4)$$

$$A = \frac{1}{\Delta T\rho c_p}\frac{P_L\tau_L}{t_m} \quad (5) \qquad A \sim \underbrace{\frac{P_L\tau_L}{t_m}}_{=:E^*} \quad (6)$$

The suitability of the parameter $E^*$, which is derived directly from the model, has already been shown in Fig. 2 for PP and ABS for an estimation of the connected area. When it is applied simultaneously to both polymers considered, a coefficient of determination $R^2$ of 0.91 is achieved in the linear regression. From this, it can be concluded that comparable processing temperatures for ABS as for PP must be addressed in the joining process. The simplifications of the model are to be taken into account, e. g. that no enthalpy of fusion is considered, and the propagation of the isotherms is considered in a simplified way. Despite the strong simplifications of the model, it provides useful information regarding the size of the connected area in the joining process.

Further information of the joining zone is obtained by microsections. Fig. 4a depicts the melted area of PP for different energies per sheet thickness. This area can be clearly determined due to the semi-crystalline character of PP. The melted area size increases with increasing $E^*$ as previously shown for the connected interface.

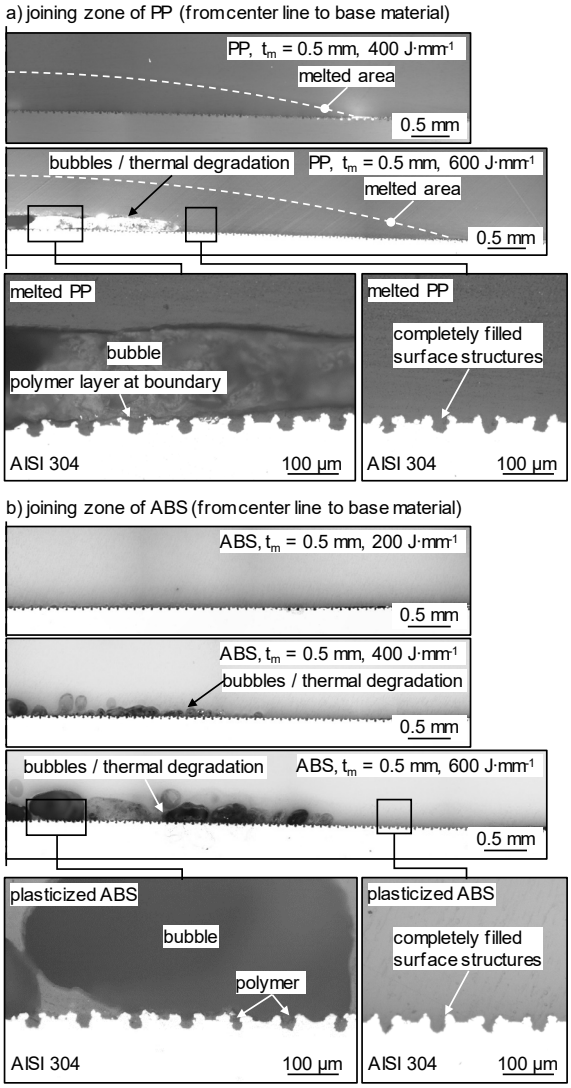


Fig. 4. Microsections from the joining zone for a) PP and b) ABS at different energies per sheet thickness E*

At the same time, bubbles occur in the middle of the joining zone with increasing energies, caused by decomposition of the polymer in the area of the highest temperatures. For all investigated parameters, the structures in the middle of the joining zone are filled with polymer completely. In the area of bubble formation, a polymer layer appears below the bubbles. In case of ABS (see Fig. 4b), a plasticized area cannot be determined easily due to the amorphous structure of the polymer. However, completely filled surface structures were determined in all cases. In contrast to PP, a larger number of smaller bubbles occur close to the interface for increasing energies. This could be explained by water-based bubble formation by moisture dissolved in ABS. Again, the bubbles are separated from the steel surface by a polymeric layer in most cases. Further information of the mentioned effects are given in [10] for bubble formation with respect to moisture and

thermal degradation as well as in [2] for structure filling depending the temperature distribution in the joining zone.

### 3.2. Mechanical properties in short-term testing

Mechanical properties were investigated based on selected parameters chosen for achieving a large connected area with simultaneous minimization of defects in the joining zone. For PP and ABS, tensile shear strengths between 15.0 up to 17.4 MPa are achieved, whereby no large effect of sheet thickness and therefore stiffness could be determined with respect to the joint strength (Fig. 5a). Furthermore, the joint failure is generally characterized by a mixed fracture with adhesive and cohesive fracture components.

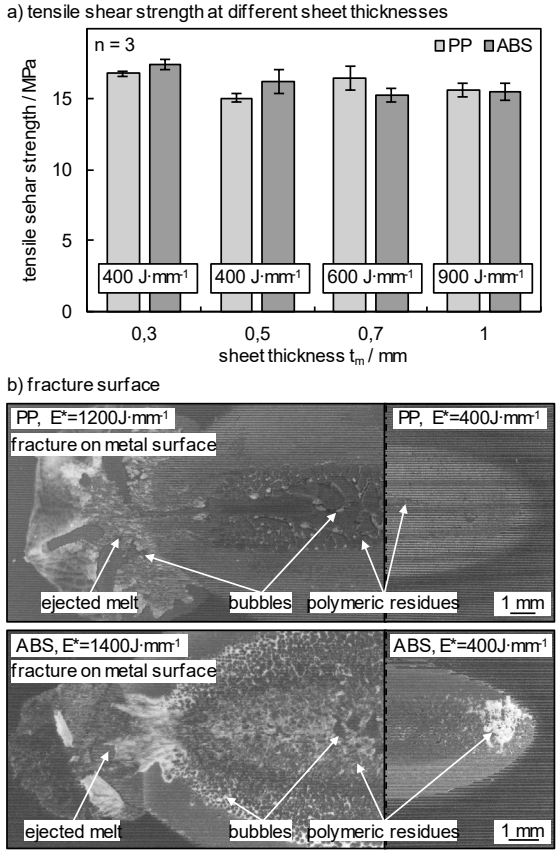


Fig. 5. a) Tensile shear strength at different sheet thicknesses and b) fracture surface at different energies per sheet thickness ($t_m$ = 0.5 mm)

Fig. 5b shows typical fracture patterns on the metal surface for different energies per sheet thickness $E^*$ and polymers (left: high $E^*$, right: low $E^*$). In case of low energies per sheet thickness, less polymer is remaining on the metal surface. By increasing the energy input, bubble formation is increased which affects the fracture behavior strongly by the failure of the polymer layer between bubbles and steel surface. Therefore, a larger amount of polymer residues at the metal surface can be determined. However, the tensile shear strength is not increased significantly because of the limitation of the load bearing cross section due to the thin polymer layer.

Furthermore, some molten polymer is ejected. The reason for melt ejection is the increase in volume with rising temperature as well as bubble formation, which displaces plasticized material [2]. In addition, it is reasonable to assume that the clamping parallel to the laser beam prevents uniform melt ejection. Therefore, the ejection occurs in the longitudinal direction of the rectangular focus.

### 3.3. Durability of the joint

Based on the described parameters, further investigations are carried out on the behavior in alternating climate test and under cyclic load.

Fig. 6a provides the results of the alternating climate test for the AISI 304-PP joints depending on the test duration and sheet thickness. The reference value represents the shown tensile shear strengths between 15 up to 17 MPa depending on the sheet thickness (see chapter 3.2). The strength of the joint decreases by up to 14 % with increasing test duration. Fig. 6b shows half of the joining zone for the reference sample and after a test time of 182 h for the metal surface as well as the joining zone (left: reference, right: after the test). On the surface of the steel, a change in the annealing colors due to corrosion can be seen. The behavior of the joining zone was monitored by photography through the opaque PP. Within the joining zone, a white seam is formed which encircles the entire connected area and indicates a uniform, circumferential detachment of the joint starting from the outside. The detachment is caused by the different thermal expansion coefficient $\alpha$ of the two materials ($\alpha_{PP} \approx 150 \cdot 10^{-6}\ K^{-1}$, $\alpha_{AISI\ 304} \approx 16 \cdot 10^{-6}\ K^{-1}$). In addition, moisture can ingress into the structures adjacent to the joining zone, expand during the temperature change and thus support the progressive damaging of the joint. Furthermore, secondary crystallization of the polymer due to ageing well above the glass transition temperature ($T_{g,PP} \approx 0$ °C) could also have an effect, since further crystallization is accompanied by shrinkage.

Fig. 6c shows the results for ABS. In principle, a comparable joint behavior can be determined. For sheet thicknesses of 0.3 and 0.5 mm the bond strength decreases by approx. 12 %. At 0.7 and 1.0 mm the result is less distinct. Due to the overlapping standard deviation no significant change can be determined, but the maximum change in tensile shear strength is also in the range of approx. 11 %. The thermal expansion of ABS is reduced compared to PP ($\alpha_{ABS} \approx 100 \cdot 10^{-6}\ K^{-1}$). However, the polymer can dissolve water, which leads to an increase in volume and thus expansion. On the other hand, secondary crystallization cannot occur due to the amorphous structure. Compared with PP, however, it cannot be stated that the different mechanisms lead to a significant change in resistance against alternating climate. Overall, the hybrid joint shows good performance compared to the climatic change test, as the loss of strength of at a maximum of approx. 14 %.

Furthermore, the fatigue behavior of the hybrid joints was investigated exemplarily for an AISI 304-PP joint with a metal sheet thickness of 0.5 mm. Fig. 7 depicts the corresponding Wöhler curve (a) as well as photographs of the joining zone at different numbers of load cycles (b). The samples were tested in natural frequency which was on average 29.80 ±0.30 Hz on average over all samples.

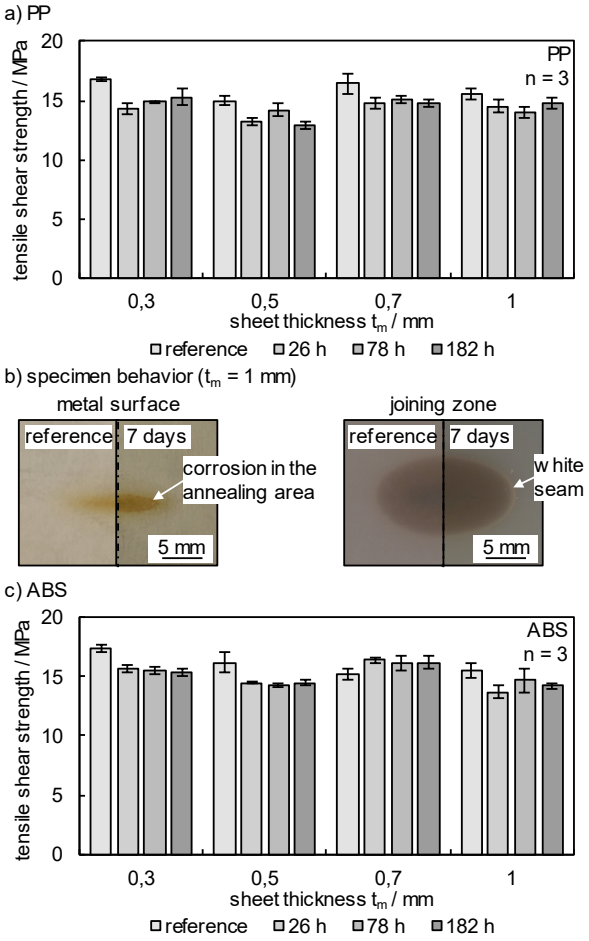


Fig. 6. Results of alternating climate test for a) AISI 304-PP joints with b) related pictures of specimens ($t_m$ = 1 mm) and c) AISI 304-ABS joints

The Wöhler curve shows a linear drop of the tensile shear load for an increasing number of cycles n. Based on the reference in the shear tensile test ($n$ = 0.5) and a strength of 15 MPa, 5 million load cycles are reliably achieved from 7 MPa onwards. This corresponds to a fatigue strength of approx. 47 % of the initial strength. Compared to other considerations in the state of the art, this value is relatively high, e.g. 35 % is achieved for ultrasonic welded AA5057-PA66CF48 joints [7]. This could be explained by the reduced stiffness of the joint due to the high-alloy steel and the non-reinforced plastic. On the other hand, a progressive damage of the joining zone can be seen starting circumferentially at the edge of the connected area, without the cracks being stopped by reinforcing materials, e.g. fibers (Fig. 7b). In the unloaded case ($n$ = 0), the joining zone shows neither visible bubbles nor other damage. A white seam forms around the circumference as the number of load cycles increases, indicating that the composite detached in this area. Therefore, the fracture occurs in the interface between both joining partners for all investigated specimens. In the region of the ejected melt (see chapter 3.2), crack growth progresses faster towards the middle of the joining zone ($n = 2.2 \cdot 10^6$). This detachment of the joining zone progresses with an increasing number of load cycles ($n = 3.8 \cdot 10^6$). This behavior is minimized by a reduction of the load.

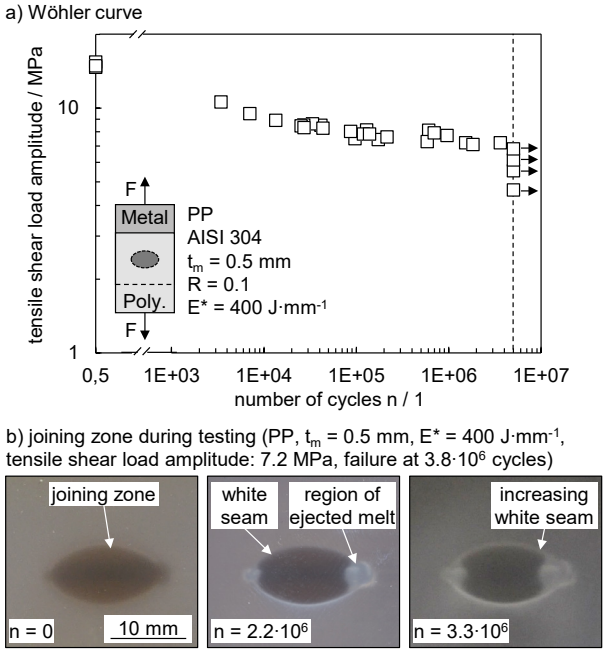


Fig. 7. a) Wöhler curve of AISI 304-PP joint and b) appearance of the joining zone during testing at different load cycles

### *3.4. Distortion of the joint*

In case of the joints between AISI 304 thin sheets and thermoplastics for domestic appliances, thermal distortion is of particular importance due to possible applications in the visible range, e.g. for panels. The investigations were applied exemplarily for ABS as polymer joining partner.

The considerations are carried out for different energies per sheet thickness $E^*$. Thereby, the material thickness $t_m$ was identified as key criterion on distortion. Further correlations to parameters of the joining process could not be determined. Fig. 8a shows the maximum distortion in z-direction for sheet thicknesses from 0.3 up to 1.0 mm as box plot. In all cases, the maximum value of the height profile was considered for the evaluation. The median as well as the upper and lower quartiles are indicated. The whisker represents the minimum respectively maximum value of the sample size. Therefore, the graph allows a wide range of $E^*$ to be considered and at the same time shows the statistical distribution of the distortion.

It can be determined that the distortion decreases with increasing sheet thickness and thus stiffness from 0.78 mm ($t_m$ = 0.3 mm) to 0.28 mm ($t_m$ = 1.0 mm). Particularly at 0.5 and 0.7 mm there is a wide spread of values. This effect occurs much more systematically at 0.5 mm, indicated by the larger area of upper and lower quartiles. At 0.7 mm, significantly more values are found in the area between the upper quartile and the maximum whisker, indicating more outliners to larger distortion. At 1.0 mm, the distortion shows less variance and reaches values between 0.22 and 0.35 mm.

Besides the maximum values, the local formation of distortion is not uniform. Fig. 8b shows a characteristic height profile for a sheet thickness of 0.3 mm and an energy per sheet thickness $E^*$ of 200 J·mm$^{-1}$. On the one hand, this illustrates that the distortion is formed around the joining zone, whereby the connected area itself gains only slight deformation due to

the solid joint bond between polymer and metal. On the other hand, the maxima form in the edge areas of the overlap. The determination of the relationships will be the focus of further investigations.

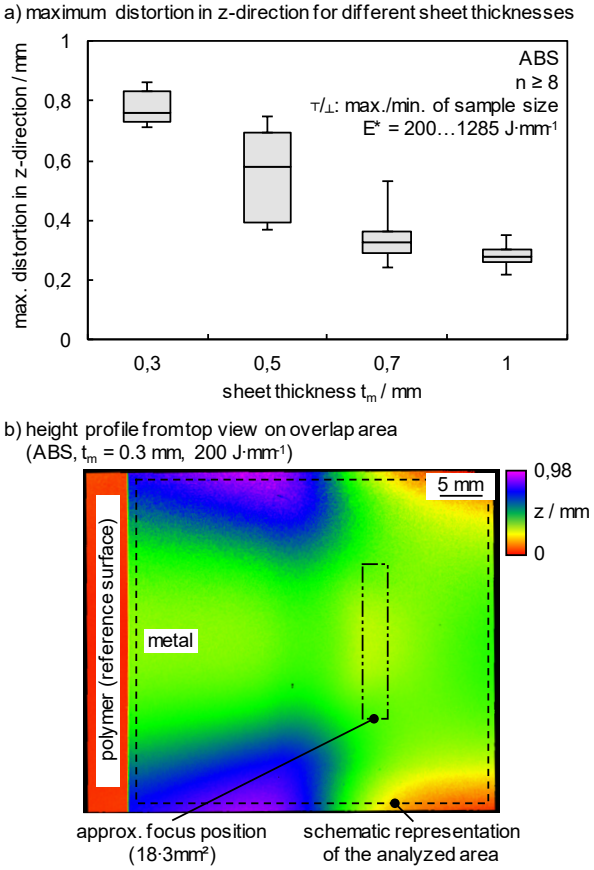


Fig. 8. a) Maximum distortion depending sheet thickness $t_m$ and b) characteristic height profile

## 4. Summary and outlook

In this paper, the joining of AISI 304 thin sheets with PP and ABS was investigated regarding the requirements of domestic appliance industry.

The growth of the connected area between polymer and metal was described by a linear correlation to the energy per sheet thickness $E^*$, which was explained by means of a simplified physical model. The appearance of the joining zone as well as the formation of voids was investigated and correlated to the fracture in mechanical testing, whereby 15.0 up to 17.4 MPa were reached as tensile shear strength. Further investigations were applied regarding the durability of the joint. An alternating climate test (-20…70 °C, 45…75 % rel. humidity, duty cycle: 26 h) led to a decrease in tensile shear strength of maximum 14 % after 182 h. In addition, fatigue strength reached approx. 47 % of the initial tensile shear strength ($R = 0.1$). Subsequently, investigations on thermal distortion were carried out, whereby a significant effect of the sheet thickness on the resulting distortion was shown which occurs strongly location dependent.

Further investigations will address distortion and its influencing variables in order to achieve a model-based description of relevant parameters. Additionally, the separation of effects regarding moisture, thermally induced expansion and secondary crystallization on the performance of the hybrid joints in alternating climate tests will be investigated.

## Acknowledgements

The project on which these results are based was supported by the Free State of Thuringia under the number 2016 FE 9077 and co-financed by European Union funds under the European Regional Development Fund (ERDF). Furthermore, the authors would like to thank G. Notni, head of Quality Assurance and Industrial Image Processing Group at Technische Universität Ilmenau, for providing the GOM Argus system as well as M. Neugebauer and M. Lüchtrath for carrying out the measurements on distortion.

## References

[1] Katayama S, Kawahito, Y., Niwa, Y, Kubota, S. Laser-Assisted Metal and Plastic Joining. Proceedings of the LANE 2007, Laser Assisted Net Shape Engineering 5, 2007, 41-51.

[2] Schricker K, Bergmann JP. Temperature- and Time-Dependent Penetration of Surface Structures in Thermal Joining of Plastics to Metals. Key Engineering Materials 809, 2019, 378-385.

[3] Schricker K, Samfaß L, Grätzel M, Ecke G, Bergmann JP. Bonding Mechanisms in Laser-Assisted Joining of Metal-Polymer Composites. Journal of Advanced Joining Processes 1, 2020, 100008.

[4] Heckert A, Zaeh MF. Laser surface pre-treatment of aluminum for hybrid joints with glass fiber reinforced thermoplastics. Journal of Laser Applications 27, 2015, S20995-1-S20995-5.

[5] Wunderling C, Scherm M, Meyer S, Zaeh MF. Thermal distortion in surface pretreatment of metal-polymer hybrids using continuous wave laser radiation. Proceeding of SPIE 10911, High-Power Laser Materials Processing: Applications, Diagnostics, and Systems VIII, 109110A, 2019.

[6] Heckert A, Singer C, Zaeh MF, Daub R, Zeilinger T. Gas-tight thermally joined metal-thermoplastic connections by laser surface pre-treatment. Physics Procedia 83, 2016, 1083-1093.

[7] Balle F, Eifler D. Monotonic and Cyclic Deformation Behavior of Ultrasonically Welded Hybrid Joints between Light Metals and Carbon Fiber Reinforced Polymers (CFRP), Fatigue Behaviour of Fiber Reinforced Polymers: Experiments and Simulations, DEStech Publications, 2012, 111-122.

[8] Goushegir SM. Friction Spot Joining of Metal-Composite Hybrid Structures. Helmholtz-Zentrum Geesthacht, Zentrum für Material- und Küstenforschung, HZG REPORT 2015-5, 2015.

[9] Schricker K. Charakterisierung der Fügezone von laserbasiert gefügten Hybridverbunden aus teilkristallinen thermoplastischen Kunststoffen und Metallen. Technische Universität Ilmenau, Fertigungstechnik – aus den Grundlagen für die Anwendung 8, 2018.

[10] Schricker K, Diller S, Bergmann JP. Bubble formation in thermal joining of plastics with metals. Procedia CIRP 74, 2018, 518-523.

[11] Schricker K., Bergmann JP. Determination of sensitivity and thermal efficiency in laser assisted metal-plastic joining by numerical simulation. Procedia CIRP 74, 2018, 511-517.